Physicochemical study of σ-bonded heteronuclear metalloporphyrin complexes of the type (P)InM(L) and (P)TlM(L) where M(L) = Mn(CO)$_5$, Co(CO)$_4$, Cr(CO)$_3$Cp, Mo(CO)$_3$Cp, or W(CO)$_3$Cp

R. Guilard *, **A. Tabard,**

Laboratoire de Synthèse et d'Electrosynthèse Organométallique associé au C.N.R.S. (U.A. 33),
Faculté des Sciences "Gabriel", 6, Boulevard Gabriel, 21100 Dijon (France)

A. Zrineh and M. Ferhat

Laboratoire de Chimie Physique Générale, Université Mohammed V, Rabat (Morocco)

(Received December 29th, 1989)

Abstract

A physicochemical study of twenty metal–metal indium and thallium porphyrins is reported. The axial metalate ligands were Mn(CO)$_5$, Co(CO)$_4$, Cr(CO)$_3$Cp, Mo(CO)$_3$Cp, and W(CO)$_3$Cp. UV-visible, ^{1}H NMR, and IR spectroscopic studies demonstrated the presence of a single metal–metal covalent bond. Infrared spectra in the carbonyl stretching region have been assigned, and values of the Cotton–Kraihanzel stretching and interaction force constants calculated, as well as the Graham σ and π parameters; these data showed that the covalent character of the metal–metal bond is strongly dependent on the nature of metals. Calculation of residual charges has shown that the thallium–manganese bond is typically covalent.

Introduction

Metalloporphyrins exhibiting metal–metal interactions have been the focus of a growing number of studies owing to their potential applications as starting materials for the preparation of new species with unusual electronic properties [1–4]. Indeed, metalloporphyrin units are present in several molecular arrangements, and donor-acceptor and σ-bonded homo- and hetero-nuclear compounds have been prepared [4,5]. In this latter series, single σ-bonded complexes with one [6–11] or two porphyrin [12] units have been described. Among the Group 13 metalloporphyrins, various indium– and thallium–metal σ-bonded heteronuclear porphyrin complexes

have been synthesized for which the porphyrin unit (OEP or TPP [13*] was coordinated to metalate anions such as $Mn(CO)_5$, $Co(CO)_4$, $Cr(CO)_3Cp$, $Mo(CO)_3Cp$, and $W(CO)_3Cp$. Surprisingly, all attempts to synthesize analogous gallium–metal complexes were unsuccessful. In order to define the influence of the porphyrin metal core on the stability of the σ metal–metal bond, we have determined and compared some physicochemical data for indium and thallium series. The UV-visible, ^1H NMR, and more particularly IR data reveal a marked variation in the nature of the σ metal–metal bond on going from the indium to the thallium complexes. The electronic properties of the metal–metal complexes in solution are considered in terms of various molecular structure parameters.

Experimental

The syntheses and handling of the metalate anions and the indium and thallium complexes were carried out under argon. Each solvent was thoroughly dried in an appropriate manner and was distilled under argon prior to use. The (P)MM'(L) complexes where P = OEP or TPP [13*] and M(L) = $Cr(CO)_3Cp$, $Mo(CO)_3Cp$, $W(CO)_3Cp$, $Mn(CO)_5$ or $Co(CO)_4$ were prepared as previously described [8,11].

Electronic absorption spectra were recorded on a Perkin–Elmer 559 spectrophotometer (solvent = benzene, concentration = 5×10^{-3} M). ^1H NMR spectra at 400 MHz were recorded on a Bruker WM 400 spectrometer of the Cerema ("Centre de Résonance Magnétique de l'Université de Bourgogne"). Spectra were recorded from C_6D_6 solutions of the complexes (5 mg) with tetramethylsilane as internal reference. Infrared spectra were recorded on a Perkin–Elmer 580 B spectrometer of samples in tetrahydrofuran.

Results and discussion

UV-visible spectroscopy

UV-visible data for all the investigated (P)InM(L) and (P)TIM(L) derivatives in benzene are summarized in Table 1. The spectra of $(OEP)InMn(CO)_5$ and $(OEP)TlMn(CO)_5$ in benzene are reproduced in Fig. 1. Each compound exhibits two bands in the Soret region and two or three Q bands in visible range. Each metal–metal complex shows an electronic absorption spectrum belonging to the hyper class [14]. Such results are in good agreement with the presence of a single σ metal–metal bond, since a similar spectral shape is observed for the σ-bonded indium– and thallium–carbon complexes [15–18].

Compared with those for the indium (P)InM(L) derivatives, the Q bands of the thallium complexes are red shifted by up to 13 nm. These absorptions correspond to $\pi-\pi^*$ transition, the $\pi \rightarrow \pi^*$ transition energy being lower for the thallium than for the indium complexes. Similar variations are observed for the tetraphenyl- and the octaethylporphyrin series. In accord with the lower basicity of the tetraphenylporphyrin ring, the Q bands of the indium and thallium octaethylporphyrin derivatives are red-shifted compared with those of the analogous tetraphenylporphyrin complexes.

As previously observed for the σ-bonded alkyl or aryl Group 13 metallo-

---

* Reference number with asterisk indicates a note in the list of references.

Table 1

UV-visible data for (P)InM(L) and (P)TlM(L) complexes in benzene (λ, nm; ϵ, $M^{-1} \cdot cm^{-1}$)

| Porphyrin, P | Axial ligand, M(L) | λ_{max} ($10^{-3}\epsilon$) | | | | | | | | | | $\epsilon(II)/\epsilon(I)$ | |
| | | Soret region | | | | Q band | | | | | | | |
| | | band I | | band II [a] | | | | | | | | | |
		In	Tl	In	Tl	In	Tl	In	Tl	In	Tl	In	Tl
TPP	Mn(CO)$_5$	387 (26.6)	358 (28.1)	457 (66.6)	457 (244.8)	544 (0.3)	548 (2.1)	586 (2.7)	592 (7.8)	633 (4.1)	638 (12.5)	2.50	8.71
	Co(CO)$_4$	369 (17.1)	352 (26.2)	446 (160.4)	452 (291.5)	534 (1.0)	540 (1.7)	575 (8.2)	584 (11.9)	618 (7.4)	626 (13.9)	9.38	11.13
	Cr(CO)$_3$Cp	393 (61.9)	360 (19.2)	459 (82.0)	458 (199.9)	547 (0.7)	548 (0.8)	588 (5.4)	593 (6.1)	636 (8.7)	649 (10.0)	1.32	10.41
	Mo(CO)$_3$Cp	383 (41.0)	354 (26.4)	457 (141.0)	458 (269.4)	542 (0.8)	548 (2.0)	587 (7.1)	594 (9.2)	634 (10.7)	640 (15.1)	3.44	10.20
	W(CO)$_3$Cp	374 (29.3)	350 (28.8)	456 (142.0)	457 (335.9)	546 (1.2)	549 (2.7)	587 (7.5)	594 (11.5)	634 (11.0)	640 (18.2)	4.85	11.66
OEP	Mn(CO)$_5$	377 (60.5)	369 (44.7)	449 (37.9)	450 (110.8)	560 (9.9)	567 (11.9)	593 (2.7)	599 (2.7)			0.63	2.48
	Co(CO)$_4$	370 (47.3)	366 (27.8)	435 (104.0)	443 (104.5)	553 (14.9)	559 (12.6)	588 (8.3)	594(5.3)			2.20	3.76
	Cr(CO)$_3$Cp	378 (74.5)	366 (43.4)	451 (42.1)	450 (97.7)	564 (14.7)	567 (13.1)	594 (3.9)	598 (2.8)			0.57	2.25
	Mo(CO)$_3$Cp	372 (58.2)	362 (38.6)	448 (61.5)	451 (145.8)	563 (13.3)	568 (15.1)	595 (3.1)	600 (2.8)			1.06	3.78
	W(CO)$_3$Cp	370 (44.6)	358 (42.3)	448 (66.1)	449 (160.4)	563 (12.9)	568 (17.6)	595 (3.2)	599 (3.8)			1.48	3.79

[a] Band B(0,0).
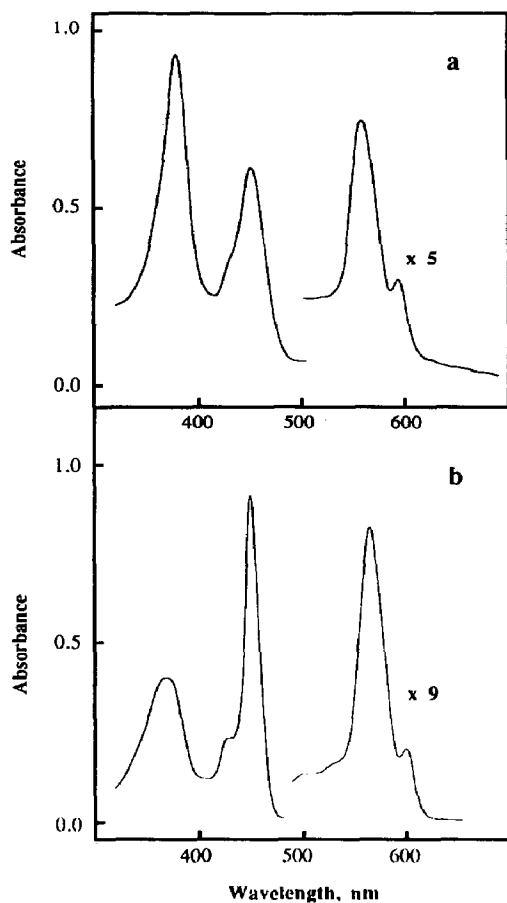
Fig. 1. Electronic absorption spectra of (a) $(OEP)InMn(CO)_5$ and (b) $(OEP)TlMn(CO)_5$ in benzene.

porphyrin series [3,15–21], the Soret band is split into two bands; band I is blue-shifted and band II red-shifted relative to those for the complexes exhibiting regular spectra. Band II appears in the same range for the both series but band I of the thallium complexes is blue-shifted compared with those for the indium analogues, the largest shifts being observed for the tetraphenylporphyrin complexes ($\Delta\lambda = 17–33$ nm). The extra band (band I) may be due to an $a_{2u}(np_z) \rightarrow e_g(\pi^*)$ transition. Such differences between the two series can be accounted for in terms of the electronegativity difference between the two metal atoms (for Tl^{III} 2.04 and In^{III} 1.78). For the octaethylporphyrin complexes, band I is blue-shifted in the indium series and red-shifted in the thallium series compared with those for tetraphenylporphyrin derivatives bearing the same axial ligand. This result can be accounted for in terms of a different dependence on the electronic properties of the porphyrin macrocycle and axial ligand of the $(P)InM(L)$ and $(P)TlM(L)$ complexes. Variations in the coordination polyhedron may also induce such changes.

Comparison of the $\epsilon(II)/\epsilon(I)$ molar absorptivity ratio is also of interest, since the degree of charge transfer from the porphyrin metal ion to the macrocycle is dependent on the electron-withdrawing character of the axial ligand, the basicity of the macrocycle, and the nature of the central metal. The values of the $\epsilon(II)/\epsilon(I)$

ratio reported in Table 1 confirm the greater electron donor ability of the oc-taethylporphyrin macrocycle and the greater electronegativity of the thallium ion, since the expected decrease and increase in the $\epsilon(II)/\epsilon(I)$ ratio are respectively observed upon going from the tetraphenylporphyrin to the octaethylporphyrin macrocycle and from the indium to the thallium as the central metal.

The shift of band I does not follow the same sequence as that for the macrocycle when a $Co(CO)_4$ anion is axially coordinated. Thus band I of $(OEP)InCo(CO)_4$ is slightly red-shifted $(\Delta\lambda = 1$ nm) compared with that of $(TPP)InCo(CO)_4$, and appears at significantly lower wavelengths than that of the corresponding tetra-phenyl- and octaethylporphyrin complexes axially coordinated to other metalate anions. The relatively weak electron-donating character of the $Co(CO)_4$ ligand may account for this result, as indicated by the high value of the $\epsilon(II)/\epsilon(I)$ ratio, the largest differences being observed for the indium series.

¹H NMR spectroscopy

Significant ¹H NMR data are summarized in Table 2; they refer to the pyrrole proton resonances for the tetraphenylporphyrin complexes and the *meso*-proton resonances for the octaethylporphyrin derivatives. Also reported are the data relating to the axial cyclopentadienyl group of the $M(CO)_3Cp$ metalate ion coordinated to the indium or thallium metal. As was the case for the UV-visible data, the NMR data indicate that the electron density on the conjugated porphyrin π system depends on the nature of porphyrin metal and the axial ligand. It has been clearly shown that the chemical shifts of the *meso* protons correlate with the central metal charge [22]. All the porphyrin proton chemical shifts are typical of a trivalent metal porphyrin. For the octaethylporphyrin derivatives, the *meso* protons of indium complexes are more deshielded than those of the thallium derivatives $(\Delta\delta \approx 0.8$ ppm). This well agrees with the UV-visible results, and implies a decrease in the electron density on the porphyrin macrocycle for the thallium series relative to that for the indium series. No such change is observed for the tetraphenylporphyrin

Table 2

¹H NMR data for (P)InM(L) and (P)TlM(L) complexes [a]

Porphyrin, P	Axial ligand, M(L)	Pyrrole or *meso* protons		Protons of axial cyclopentadienyl group	
		δ(In)	δ(Tl)	δ(In)	δ(Tl)
TPP	Mn(CO)₅	9.09	9.09		
	Co(CO)₄	9.10	9.09 (23) [b]		
	Cr(CO)₃Cp	9.08	9.09	1.84	1.86
	Mo(CO)₃Cp	9.09	9.10	2.59	2.50
	W(CO)₃Cp	9.09	9.10	2.53	2.48
OEP	Mn(CO)₅	10.45	10.36		
	Co(CO)₄	10.48	10.42 (22) [b]		
	Cr(CO)₃Cp	10.45	10.37	1.63	1.64
	Mo(CO)₃Cp	10.45	10.38	2.39	2.32
	W(CO)₃Cp	10.43	10.37	2.35	2.30

[a] Spectra recorded in C_6D_6 at 294 K with $SiMe_4$ as internal reference; chemical shifts $(\delta$, ppm) downfield from $SiMe_4$ are defined as positive. [b] Values in parentheses are ¹H–²⁰³,²⁰⁵Tl coupling constants in Hz.

derivatives. Possibly owing to the change in the ring current, the pyrrole proton chemical shifts are not very dependent on the porphyrin electron density charge.

As suggested by the UV-visible data, the $(P)MCo(CO)_4$ complexes present typical behavior. The *meso* protons of the octaethylporphyrin complexes are more de-shielded and a $^1H-^{203,205}Tl$ coupling constant is observed. This result can only be attributed to the strongly electron-withdrawing ability of the $Co(CO)_4$ metalate anion. An other characteristic of the $(P)MM'(CO)_n$ derivatives is the weak inequivalence of the two porphyrin faces compared with that for the $(P)MM'(CO)_3Cp$ and (P)MR [15–18] complexes (Fig. 2). Such behaviour has been reported previously for the trinuclear indium complexes [12] in which a $Fe(CO)_4$ group is σ-bonded to two (OEP)In units, and the symmetry of the axial ligand was invoked to account for this since no solvent effect was observed. The IR data described below confirm this hypothesis. The other factor responsible for the porphyrin anisotropy is the distance of the metal from the porphyrin mean plane ($\Delta 4N$). The X-ray data are also in good accord with the NMR studies, since the metal is close to the porphyrin plane when a $Mn(CO)_5$ ligand is coordinated to the thallium or indium atom ($\Delta 4N(In-Mo(CO)_3$ Cp) 0.791(1) Å [24], $\Delta 4N(In-Mn(CO)_5)$ 0.744(1) Å [8], $\Delta 4N(Tl-Mo(CO)_3Cp)$ 1.000(1) Å [25], $\Delta 4N(Tl-Mn(CO)_5)$ 0.939(1) Å [11]).

No significant change is observed in the porphyrin proton resonances when the Cr metal is replaced by the Mo or W atom, but the axial cyclopentadienyl protons of the $Cr(CO)_3Cp$ group are more shielded than those of the $M(CO)_3Cp$ ligand where M = Mo or W. King reported that the π-cyclopentadienyl chemical shift can be used to define the nature of the bonding between the cyclopentadienyl group and the metal atom [23]. No similar relationship has been found for the investigated metalloporphyrin series. Only the shielding of the $(P)MCr(CO)_3Cp$ axial protons can be interpreted in terms of the cyclopentadienyl displacement towards the
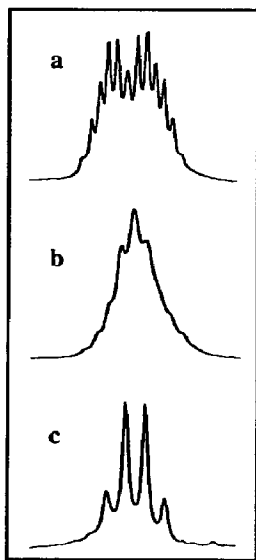

Fig. 2. ^1H NMR resonances of the methylenic protons for the (OEP)TlM(L) complexes where M(L) = (a) $Cr(CO)_3Cp$, (b) $Co(CO)_4$, (c) $Mn(CO)_5$ (C_6D_6, 294 K).

porphyrin ring leading to a shorter porphyrin–cyclopentadienyl distance. The small changes in the cyclopentadienyl proton chemical shift observed for the indium and thallium complexes demonstrate that the mean cyclopentadienyl–porphyrin distance is close for the two series. The X-ray structure studies of $(OEP)InMo(CO)_3Cp$ and $(OEP)TlMo(CO)_3Cp$ support this suggestion, since a larger metal–porphyrin distance and a smaller cyclopentadienyl–porphyrin dihedral angle are observed for the thallium derivatives [24,25]. As expected, the octaethylporphyrin macrocycle induces a larger shielding of the cyclopentadienyl protons than the tetraphenylporphyrin ring.

IR Spectroscopy

The above study demonstrates that the cyclopentadienyl proton resonances are strongly dependent on the nature of the porphyrin macrocycle and slightly on the metal electronegativity. The IR data should be more sensitive to changes of structural arrangement and metal–metal bond electronic properties, and a study of the CO vibrations was thus of interest.

The $\nu(CO)$ frequencies and mode attributions for the twenty investigated complexes are summarized in Table 3. Two or three bands are observed in tetrahydrofuran solution (Fig. 3). This is consistent with the local symmetry of the metalate ligands $(Mn(CO)_5: C_{4v}, 2A_1 + E + B_1; Co(CO)_4: C_{3v}, 2A_1 + E; M(CO)_3Cp$ (M = Cr, Mo, W): $C_s, 2A' + A'')$. The assignment was carried out by taking account of the calculated force constants (Table 3) determined by the Cotton–Kraihanzel method [26–28]. The $(P)MMn(CO)_5$ complexes show only two CO stretching bands because the A_1 and E modes overlap, the B_1 mode being non-infrared active. As already deduced from the ^1H NMR data, the axial ligand symmetry is not dependent on the porphyrin metal.

A significant shift of the CO stretching modes towards low wavenumbers is observed on going from the tetraphenylporphyrin to the octaethylporphyrin series.
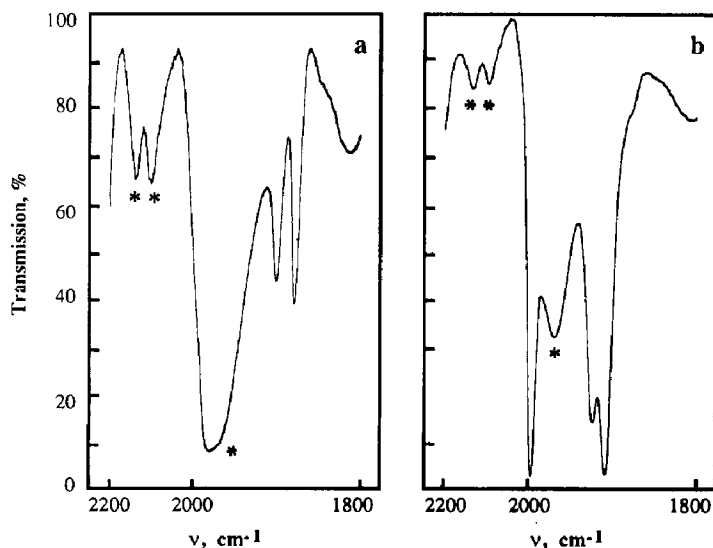

Fig. 3. IR spectra in the CO stretching region of (a) $(TPP)InW(CO)_3Cp$ and (b) $(TPP)TlW(CO)_3Cp$ in tetrahydrofuran solution (the bands labelled (*) are due to the solvent).

Table 3

$\nu(CO)$ wavenumbers, force constants [29*] and Graham parameters for the (P)InM(L) and (P)TlM(L) complexes in tetrahydrofuran solution

Porphyrin, P	Axial ligand, M(L)	Porphyrin metal	$\nu(CO)$ (cm^{-1})			average value, $\nu(CO)_m$	Force constants (10^5 dyn cm^{-1})			Graham parameters (10^5 dyn cm^{-1})		Residual charge (electron)
			ν_1	ν_2	ν_3		k_1	k_2	k^d	$\Delta\sigma^e$	$\Delta\pi^e$	
TPP	Mn(CO)$_5$	In	2078 (A$_1$)	1974 (A$_1$,E)		2000 ^{a}	15.91	16.25	0.26	−0.94	0.37	0.11
		Tl	2092 (A$_1$)	1998 (A$_1$,E)		2021 ^{a}	16.28	16.59	0.23	−0.63	0.40	≈ 0
	Co(CO)$_4$	In	2070 (A$_1$)	1999 (A$_1$)	1970 (E)	2002 ^{b}	16.76	16.00	0.33	−1.14	0.35	0.26
		Tl	2079 (A$_1$)	2016 (A$_1$)	1989 (E)	2018 ^{b}	16.99	16.27	0.30	−0.83	0.31	0.16
	Cr(CO)$_3$Cp	In	1967 (A$'$)	1902 (A$'$)	1872 (A$''$)	1914 ^{c}	14.68	14.85	0.70	−1.00	0.25	0.30
		Tl	1983 (A$'$)	1924 (A$'$)	1908 (A$''$)	1938 ^{c}	15.12	15.21	0.51	−0.72	0.33	0.14
	Mo(CO)$_3$Cp	In	1980 (A$'$)	1905 (A$'$)	1882 (A$''$)	1922 ^{c}	14.88	14.95	0.65	−1.09	0.24	0.27
		Tl	1999 (A$'$)	1933 (A$'$)	1915 (A$''$)	1949 ^{c}	15.28	15.38	0.57	−0.63	0.21	0.09
	W(CO)$_3$Cp	In	1976 (A$'$)	1898 (A$'$)	1875 (A$''$)	1916 ^{c}	14.77	14.87	0.67	−1.06	0.25	0.27
		Tl	1996 (A$'$)	1923 (A$'$)	1907 (A$''$)	1942 ^{c}	15.12	15.29	0.61	−0.57	0.18	0.10
OEP	Mn(CO)$_5$	In	2075 (A$_1$)	1972 (A$_1$,E)		1998 ^{a}	15.87	16.21	0.25	−0.98	0.37	0.12
		Tl	2087 (A$_1$)	1996 (A$_1$,E)		2019 ^{a}	16.24	16.54	0.23	−0.69	0.41	≈ 0
	Co(CO)$_4$	In	2066 (A$_1$)	1999 (A$_1$)	1969 (E)	2001 ^{b}	16.78	15.97	0.31	−1.22	0.40	0.27
		Tl	2074 (A$_1$)	2008 (A$_1$)	1988 (E)	2015 ^{b}	16.76	16.27	0.31	−0.60	0.08	0.18
	Cr(CO)$_3$Cp	In	1964 (A$'$)	1892 (A$'$)	1873 (A$''$)	1910 ^{c}	14.65	14.77	0.61	−1.13	0.30	0.32
		Tl	1979 (A$'$)	1917 (A$'$)	1907 (A$''$)	1934 ^{c}	14.98	15.18	0.49	−0.64	0.22	0.17
	Mo(CO)$_3$Cp	In	1976 (A$'$)	1899 (A$'$)	1882 (A$''$)	1919 ^{c}	14.76	14.93	0.63	−1.01	0.14	0.29
		Tl	1995 (A$'$)	1926 (A$'$)	1916 (A$''$)	1946 ^{c}	15.14	15.37	0.54	−0.51	0.08	0.11
	W(CO)$_3$Cp	In	1973 (A$'$)	1892 (A$'$)	1877 (A$''$)	1914 ^{c}	14.65	14.85	0.65	−0.98	0.15	0.29
		Tl	1991 (A$'$)	1917 (A$'$)	1907 (A$''$)	1938 ^{c}	15.01	15.26	0.58	−0.52	0.10	0.12

^{a} $\nu(CO)_m = \frac{1}{4}(\nu_1 + 3\nu_2)$. ^{b} $\nu(CO)_m = \frac{1}{4}(\nu_1 + \nu_2 + 2\nu_3)$. ^{c} $\nu(CO)_m = \frac{1}{3}(\nu_1 + \nu_2 + \nu_3)$. ^{d} k = interaction constant (approximations: M(L) = Mn(CO)$_5$, $k = k_c = k'_c = k_t/2$ [27]; M(L) = Co(CO)$_4$, $k = k_c = k_t$ [28]; M(L) = M(CO)$_3$Cp where M = Cr, Mo or W, $k = k_d = 2k_s$ [28,30]. ^{e} Reference compounds are (CH$_3$)M(L) [30,31].

Such a change indicates that the tetraphenylporphyrin unit lowers the charge on the axial ligand. This feature, already revealed by UV-visible spectroscopy, can account for the lower stability of the tetraphenylporphyrin complexes. Another significant trend is that the stretching force constants increase and the interaction constants decrease when the indium atom is replaced by the thallium atom. This confirms the UV-visible results, and unambiguously demonstrates that the electronegativity of thallium is higher than that of indium. The stretching force constants also depend on the nature of the axial metal. Thus the highest k_1 values are observed when the $Co(CO)_4$ group is the axial ligand and the lowest one is observed for the $(P)MCr(CO)_3Cp$ derivatives. To define the σ and π donor or acceptor character of the axial and equatorial units, the σ and π parameters were calculated according from the following equations [31]:

$$\Delta k_1 = \Delta\sigma + k_d/k_s \, \Delta\pi$$

$$\Delta k_2 = \Delta\sigma + \Delta\pi$$

The σ and π parameters for the twenty investigated complexes (Table 3) were determined by using the $(CH_3)ML$ derivatives as references. The π parameters show that the $(P)M$ unit has a π electron-withdrawing character, and the highly negative σ parameters indicate a strong σ donor character, the highest one being observed for the $(OEP)InCo(CO)_4$ complex. This later finding agrees well with that from the UV-visible study. As expected, the σ parameters of the thallium complexes are closer to those of the reference compounds than are the indium derivatives.

The meaning of the sequence determined in the nature of the axial ligand is not clear, and it seemed of interest to compare the derivatives possessing the axial $M(CO)_3Cp$ unit. These axial ligands show a σ electron-donor character, leading to a greater electron density on the cyclopentadienyl ligand. This causes a decrease in the σ and π bonding strength, and an increase in the cyclopentadienyl ring–axial metal δ bonding strength. The shielding of the $Cr(CO)_3Cp$ proton chemical shift confirms this interpretation.

The residual charge on the axial metalate ligand can be determined from the average frequency [32]. The data given in Table 3 show that the average frequencies of the porphyrin complexes correspond to values intermediate between those for the corresponding metalate anions and dimers [33*], for which the residual charge is 1 and 0 electron, respectively. Indeed, the calculated residual charges for the investigated complexes are in the range 0.32–0. Such data are typical of a covalent metal–metal bond, and clearly demonstrate that the degree of covalent bond character only depends on the nature of the metals. The data also show that the Tl–Mn bond is the more covalent, and the In–Cr bond the more polarized. Surprisingly, the nature of the metal–metal bonding is similar in the molybdenum and tungsten complexes. The scheme below presents a comparison of the residual charge for the indium and thallium derivatives having the same metalate group as the axial ligand. The residual charge is about three times as large for the indium complexes than for the thallium compounds.

This study has unambiguously revealed the various parameters that influence the character of the axial metal–metal bond in heterobimetallic porphyrins, and can be used to predict the stabilities of such complexes. We can now understand why all attempts to synthesize analogous gallium porphyrin complexes were unsuccessful. The findings detailed in this paper form the basis of research now in progress aimed at preparing new stable metal–metal porphyrins.

References

1 J.A. Ibers, L.J. Pace, J. Martinsen and B.M. Hoffman, Struct. Bonding, 50 (1982) 1.
2 J.S. Miller (Ed.), Extended Linear Chain Compounds, Plenum Press, New York, 1982.
3 R. Guilard, C. Lecomte and K.M. Kadish, Struct. Bonding, 64 (1987) 205.
4 R. Guilard and K.M. Kadish, Comments Inorg. Chem., 7 (1988) 287.
5 P.J. Brothers and J.P. Collman, Acc. Chem. Res., 19 (1986) 209.
6 P. Cocolios, C. Moïse and R. Guilard, J. Organomet. Chem., 228 (1982) C43.
7 P. Cocolios, D. Chang, O. Vittori, R. Guilard, C. Moïse and K.M. Kadish, J. Am. Chem. Soc., 106 (1984) 5724.
8 R. Guilard, P. Mitaine, C. Moïse, C. Lecomte, A. Boukhris, C. Swistak, A. Tabard, D. Lacombe, J.-L. Cornillon and K.M. Kadish, Inorg. Chem., 26 (1987) 2467.
9 H.W. Bosch and B.B. Wayland, J. Organomet. Chem., 317 (1986) C5.
10 T. Boschi, S. Licoccia, R. Paolesse and P. Tagliatesta, Inorg. Chim. Acta, 145 (1988) 19.
11 R. Guilard, A. Zrineh, M. Ferhat, A. Tabard, P. Mitaine, C. Swistak, P. Richard, C. Lecomte and K.M. Kadish, Inorg. Chem., 27 (1988) 697.
12 R. Guilard, P. Mitaine, C. Moïse, P. Cocolios and K.M. Kadish, New J. Chem., 12 (1988) 699.
13 The investigated porphyrins, P where P = OEP^{2-} and TPP^{2-} are the dianions of octaethylporphyrin and tetraphenylporphyrin, respectively.
14 M. Gouterman, in D. Dolphin (Ed.), The Porphyrins, Vol. III, Academic Press, New York, 1978, Ch. 1 and ref. therein.
15 P. Cocolios, R. Guilard and P. Fournari, J. Organomet. Chem., 179 (1979) 311.
16 K.M. Kadish, B. Boisselier-Cocolios, P. Cocolios and R. Guilard, Inorg. Chem., 24 (1985) 2139.
17 A. Tabard, R. Guilard and K.M. Kadish, Inorg. Chem., 25 (1986) 4277.
18 K.M. Kadish, A. Tabard, A. Zrineh, M. Ferhat and R. Guilard, Inorg. Chem., 26 (1987) 2459.
19 R. Guilard, A. Zrineh, A. Tabard, A. Endo, B.C. Han, C. Lecomte, M. Souhassou, A. Habbou, M. Ferhat and K.M. Kadish, submitted.
20 A. Coutsolelos and R. Guilard, J. Organomet. Chem., 253 (1983) 273.
21 K.M. Kadish, B. Boisselier-Cocolios, T. Coutsolelos, P. Mitaine and R. Guilard, Inorg. Chem., 24 (1985) 4521.
22 H. Scheer and J.J. Katz in K.M. Smith (Ed.), Porphyrins and Metalloporphyrins, Elsevier, Amsterdam, 1975, Chapter 10.
23 R.B. King, Inorg. Chim. Acta, 2 (1968) 454.
24 C. Lecomte, A. Habbou, P. Mitaine, P. Richard and R. Guilard, Acta Cryst. C, 45 (1989) 1226.
25 P. Richard, A. Zrineh, R. Guilard, A. Habbou and C. Lecomte, Acta Cryst. C, 45 (1989) 1224.
26 P. Braunstein and J. Dehand, J. Organomet. Chem., 81 (1974) 123.
27 F.A. Cotton and C.S. Kraihanzel, J. Am. Chem. Soc., 84 (1962) 4432.
28 P. Braunstein and J. Dehand, Bull. Soc. Chim. Fr. (1975) 1997.
29 For $M(L) = Mn(CO)_5$ or $Co(CO)_4$, k_1 and k_2 are the axial and equatorial CO stretching force constants, respectively; k_c, k'_c and k_t are the interaction constants relative to the axial–equatorial and equatorial–equatorial CO groups, respectively. For $M(L) = M(CO)_3Cp$ where M = Cr, Mo, or W, k_1 and k_2 represent the two stretching force constants of carbonyl groups which are diagonal to the (P)In or (P)Tl unit; k_d and k_s are the carbonyl diagonal and lateral interaction force constants, respectively.
30 R.B. King and L.W. Houk, J. Can. Chem., 47 (1969) 2959.
31 W.A.G. Graham, Inorg. Chem., 7 (1968) 315.
32 O. Kahn and M. Bigorgne, J. Organomet. Chem., 10 (1967) 137.
33 $\nu(CO)_m(Mn(CO)_5^-)$ 1863, $\nu(CO)_m(Mn_2(CO)_{10})$ 2017, $\nu(CO)_m(Co(CO)_4^-)$ 1885, $\nu(CO)_m(Co_2(CO)_8)$ 2044, $\nu(CO)_m(Cr(CO)_3Cp^-)$ 1811, $\nu(CO)_m([Cr(CO)_3Cp]_2)$ 1959, $\nu(CO)_m(Mo(CO)_3Cp^-)$ 1812, $\nu(CO)_m([Mo(CO)_3Cp]_2)$ 1962, $\nu(CO)_m(W(CO)_3Cp^-)$ 1810, $\nu(CO)_m([W(CO)_3Cp]_2)$ 1956 cm^{-1}.